J Mater Sci (2007) 42:9671–9678
DOI 10.1007/s10853-007-1961-7

The shock response, simulation and microstructural determination of a model composite material

Samuel Alan McDonald · Jeremy C. F. Millett · Neil K. Bourne · Keith Bennett · Alec M. Milne · Philip J. Withers

Received: 12 February 2007 / Accepted: 21 June 2007 / Published online: 30 July 2007

Abstract The capability to assess microstructural details in a polymer matrix composite is important in addressing composite design for engineering applications. The generation of three-dimensional microstructure using a non-invasive high-resolution experimental diagnostics method will advance our knowledge within this field. An inert composite has been studied, and both X-ray microtomography (XRT) for microstructural investigation in 3D and a parallel series of shock experiments (with associated modelling) have been conducted. The experimental aims of this study lay in several areas: firstly, to adequately define the bulk morphology; secondly, to determine the geometry of defects within the material; and finally, to demonstrate a direct linkage with the mechanical response determined by finite element analysis. This work is the first step in finding a way to non-invasively link 3D microstructural invesigation and numerical simulation to predict the shock performance of a composite material.

S. A. McDonald (✉) · P. J. Withers
Materials Science Centre, School of Materials, University of Manchester, Grosvenor Street, Manchester M1 7HS, UK
e-mail: sam.mcdonald@manchester.ac.uk

J. C. F. Millett
AWE, Aldermaston, Reading, Berkshire RG7 4PR, UK

N. K. Bourne
School of Aerospace, Mechanical and Civil Engineering, University of Manchester, Sackville Street, Manchester M60 1QD, UK

K. Bennett · A. M. Milne
Fluid Gravity Engineering, 83 Market Street, St. Andrews, Fife KY16 9NX, UK

Introduction

Understanding the response of energetic materials, such as plastic bonded explosives (PBXs), to high strain rate loading is of concern given that this can result in hot spots that can ultimately lead to a violent reaction. The response of such composite materials to purely mechanical loading (particularly shock loading) is therefore of interest from a safety point of view. Thus, one of the largest focuses of research into the high-strain-rate response of polymer-based composites has been in the explosives community. The dynamic behaviour of any composite material (energetics included), is related to its bulk morphology and the behaviour of each of the individual phases contained within. It is important, therefore, to investigate and define the microstructure of the material. For example, a unidirectional fibre composite will have a pronounced anisotropy in its mechanical properties [1]. Microstructural investigation is necessary both to understand detail of the fines present within the binder phase, and also to define the form of defects such as voids or cracks that might lead to hot spots by collapse or shear. The resolution of details of the microstructure in energetic materials has important applications in addressing safety issues that relate to their production and handling. Increased resolution will enable operating mechanisms of interest to be studied at the appropriate length scales.

While energetic composites consist of particulate explosive crystals bound in an inert or energetic polymer binder phase, and thus can be considered to be macroscopically isotropic, the size and distribution of the particles have been shown to affect the overall mechanical behaviour [2, 3]. In a sugar-based mock explosive, Millett and Bourne found the particle size to have a significant effect upon the Hugoniot in terms of stress and particle velocity (all other conditions being identical), with the

material possessing the larger particle size having the steeper Hugoniot [2]. In exploring the issue of particle size further, in a soda-lime glass-hydroxyterminated polybutadiene (HTPB) binder composite system, Millett et al. again found the measured shock stresses to demonstrate that the Hugoniot is sensitive to particle size, with the largest particles generating the highest stresses [3]. It is clear that it is important to adequately describe the microstructure of the material and understand its response, particularly at the length-scales of importance, in order to assess potential hazards in a particular geometry.

X-ray microtomography (XRT) is a non-destructive evaluation technique that allows the internal structure of an object/sample to be imaged by reconstructing the spatial distribution of the local linear X-ray absorption coefficients of the materials/phases contained within [4–6]. This provides a virtual, three-dimensional representation of the interior of the object from which two-dimensional cross-sectional slices can be viewed through the three orthogonal directions of the volume. In conventional radiography, the image plane is approximately normal to the X-ray beam, and the image represents total X-ray attenuation through the object. Computed tomography (CT) creates a digital representation of a thin slice of the object parallel to the X-ray beam. This image is reconstructed from a series of two-dimensional radiographs taken at different orientations. The CT slice is stored as an array of numbers representing local X-ray attenuation values for each of the small volume elements (voxels) that make up the slice, and represented in a reconstructed image as a series of grey level values. The work discussed in this paper centres around the microstructural investigation of a composite material. Putting it in the context of that of Baer and Trott [7], Trott et al. [8] and Mas and Clements [9] in terms of the mesoscale modelling of composites, linking the three dimensional microstructural data obtained directly to simulation codes can lead to a computational design capability.

A soda-lime glass, hydroxy-terminated polybutadiene (HTPB) composite system has been studied, for which the shock response of both materials has been determined [10, 11]. As spheres, the glass particles have a well-controlled geometry and a bimodal distribution of particle sizes with narrow size ranges was used for the manufacture of the composite material used in this work. An integrated approach linking testing, modelling and microstructural investigation has been taken to understand the response of real systems.

Experimental

Materials

For the glass-binder composite system, soda-lime glass spheres, obtained from Boud Marketing Limited, were sieved to provide average particle size distributions of 300 and 30 μm, and a composite containing equal proportions of the coarse and fine spheres was made. The HTPB binder system has been studied previously [10]. It consisted of 88 parts of HTPB to 12 parts of isophorone diisocyanate (IPDI) by weight, with 0.05 parts of dibutyl tin laureate as a catalyst. These were mixed with 60 wt.% of the glass spheres and cured at 60 °C for 1 week. Material properties for the HTPB and the soda-lime glass are given in Table 1. In terms of the Hugoniots of the components of the composite, it has been shown that the equation of state of soda-lime glass is considerably steeper than that of the HTPB [3]. Given that the Hugoniot elastic limit of soda-lime glass is ca. 6 GPa [11], it would be expected in the plate impact experiments that the glass will behave elastically, and thus inelastic deformation will be concentrated in the HTPB binder.

X-ray microtomography

Measurements were carried out using a high-resolution, computerised tomography and digital radiography system (HMXST 225), from X-Tek Systems Ltd., employing a microfocus X-ray source (5 μm focal spot size) capable of tube potentials up to 225 kV. The imaging arrangement in this system was based on the cone beam geometry, as illustrated in Fig. 1. In using such a geometry, the voxel resolution of the reconstructed 3D volume depends on the source-to-object distance. The sample was placed on an object manipulator situated between the X-ray source and the detector system (consisting of image intensifier and CCD), providing magnification and rotation for collection of radiographs over 180°. For the purpose of the material investigated in this study, owing to a relatively low X-ray absorption, a tube potential of 50 kV was used with a copper anode target. This, in conjunction with the use of a beryllium windowed detector, ensured attenuation of the X-rays through the polymer matrix composite material. In order to shape the energy spectrum of the X-ray source, and thus improve the image quality in the reconstructed slices by increasing the signal-to-noise ratio, a 0.1 mm thick

Table 1 Material properties of the composite constituents

Material	ρ (g cm^{-3})	c_0 (mm μs^{-1})	S	Z ρc_L	c_L (mm μs^{-1})	c_S (mm μs^{-1})	v	HEL (GPa)
HTPB	0.93	1.53	2.84	1.36	1.46	1	0.06	0.1
Soda-lime glass	2.49	4.27	0.8	14.54	5.84	3.46	0.23	6.0

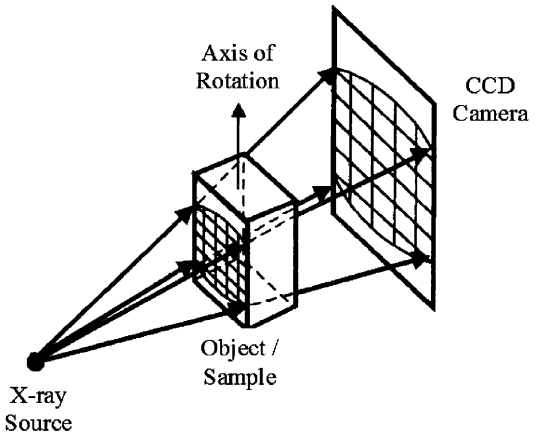

Fig. 1 Schematic diagram of the laboratory X-ray microtomography setup used in the experimental work, and in particular the cone beam arrangement

aluminium filter was placed in front of the sample during image acquisition. The effect of such an X-ray filter is to remove low-energy photons from the polychromatic beam, thus minimising artefacts in the reconstructed slices and the distribution of voxels with different intensities. Filtration of the beam prior to attenuation through the object thus gives a more uniform distribution of voxel intensities and reduces noise. The 3D tomographic volumes were reconstructed using a cone beam extension of the filtered back-projection algorithm for fan beams [12] from 470 radiographs acquired using a sample rotation step of 0.4°, with 32 frames averaged for acquisition of each projection (using an exposure time for each frame of 120 ms).

Tomographic measurements were performed on 5 mm diameter spherical or 5 mm cubed pieces of the composite material both before and after the shock tests had been carried out. The sample used for tomography analysis prior to the shock tests, and that used as input to the hydrocode, was taken from the central region of the cup in order to eliminate all edge effects. For the shocked sample, the investigated pieces were cut from different locations to ensure that a full picture of the damage mechanisms taking place was achieved, enabling the evolution of the microstructure of the material to be determined.

Shock testing

Plate impact experiments were performed to determine the shock response of the composite material using a 50 mm bore, 5 m single-stage gas gun [13, 14]. This involved the measurement of the Hugoniot in terms of the shock (impact) stress, shock velocity and the particle velocity. The composite was cast into a dural (aluminium alloy 6082-T6) cup of inner diameter 80 mm by 11 mm deep. The base of each cup consisted of a 1 mm thick plate which had been machined flat and parallel to within ± 5 μm. Accuracy of thickness of the composite samples was maintained by casting into an accurately machined frame that was placed over the stress-gauged plate. A manganin stress gauge (MicroMeasurements type LM-SS-125CH-048) was fixed to the inner face of the cup base, with a 25 μm thick sheet of Mylar on either side of the gauge to provide electrical insulation. In preparing the target assembly in this manner, an accurate specimen could be made without the need for the complicated cooling arrangements using liquid nitrogen that are required to machine these highly compliant (rubbery) materials. By placing the stress gauge at the interface between the cover plate and the composite target material, and matching the flyer plate to the cover plate, the gauge itself would record the internal stress generated by the impact, as dictated by the initial conditions. This method has been used successfully to measure the shock response of soda-lime glass-HTPB composites [3] and cyclotrimethylene trinitramine (RDX)-based plastic-bonded explosive and sugar-based simulants [2]. It is also a variant of a technique demonstrated successfully on a number of other materials, including HTPB [10] and the elastomer polychloroprene [15]. A second stress gauge was supported on the back of the composite target assembly with a 12 mm thick block of polymethylmethacrylate. In this way, the two gauges mounted in the assembly allowed not only the shock stress to be measured directly (from the amplitude of the signal), but, through the known separations of the gauges in terms of position within the target assembly (Δw) and time (Δt_{shock}), the shock velocity ($U_s = \Delta w/\Delta t_{\text{shock}}$) was determined as well. Shock stresses were imposed by the impact of a 10 mm dural flyer plate at a velocity of 437 m s^{-1} (for the shot for which gauge trace data is reported in this work). Impact velocities were measured from the electrical shorting of sequentially mounted pairs of pins to an accuracy of ca. 0.1%. Voltage data from the gauges were converted to stress according to the methods of Rosenberg et al. [16]. The flyer plate material was chosen such that it matched the material of the plate on which the composite sample had been cast. Particle velocities (u_p), that is the velocity of material flow behind the shock front, were determined from the measured longitudinal Hugoniot stresses (σ_x) and the measured impact velocities and known response of the flyer plate material [17] using impedance matching techniques. A schematic diagram of the specimen assembly and gauge placements is shown in Fig. 2.

In the regimes chosen for investigation the binder phase yields inelastically but the glass filler phase is within its elastic regime. A similar material has been recovered and examined and the following observations were noted [3]. The glass spheres show no signs of damage. The binder phase was seen to have delaminated from the spheres and

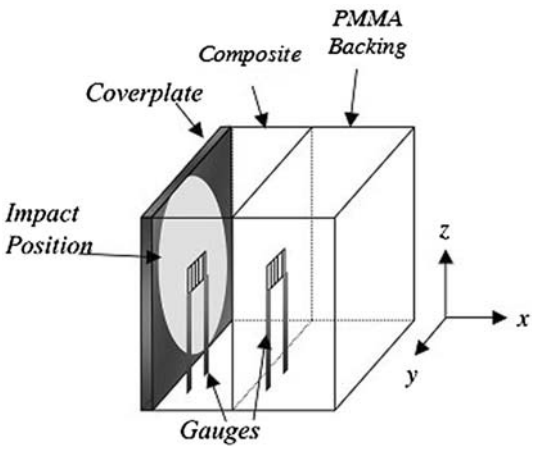

Fig. 2 Illustrating the sample configuration and gauge placement for the impact tests

there was some evidence of apparent flow of the binder around the glass inclusions.

Numerical simulations

The 3D tomographic datasets were read directly into the mesh generators for three-dimensional simulation, such that the actual microstructure of the material was being modelled. The code employed was an Eulerian, multimaterial hydrocode, Eden [18]. The material descriptions employed a Murnaghan equation of state and an elastic-perfectly plastic constitutive description. The simulation had a reverse ballistic geometry and consisted of essentially impacting onto a rigid boundary which was across its base plane. The grey level data represented by each voxel within the tomographic reconstruction is on a linear scale and proportional to the mass of the material contained in the voxel at that spatial position within the sample. From the known ingredient densities and the measured mixture density [3] volume fraction distributions of the glass and HTPB binder components were produced. It is important with tomographic data that care is taken to ensure accurate reconstruction of an interface between glass and binder when thresholding. Threshold contours were invoked to identify edges between a sphere and the binder which were then varied within narrow bands to ensure that the calculated mixture density matched the actual value.

Results and discussion

Initial XRT

Figure 3 shows virtual greyscale slices extracted from the three orthogonal directions of the reconstructed 3D volume of the glass composite material prior to the shock tests. A number of observations can be made from the tomographic images regarding the microstructure of the material. The glass spheres are clearly resolved and are uniformly distributed throughout the material—both the larger

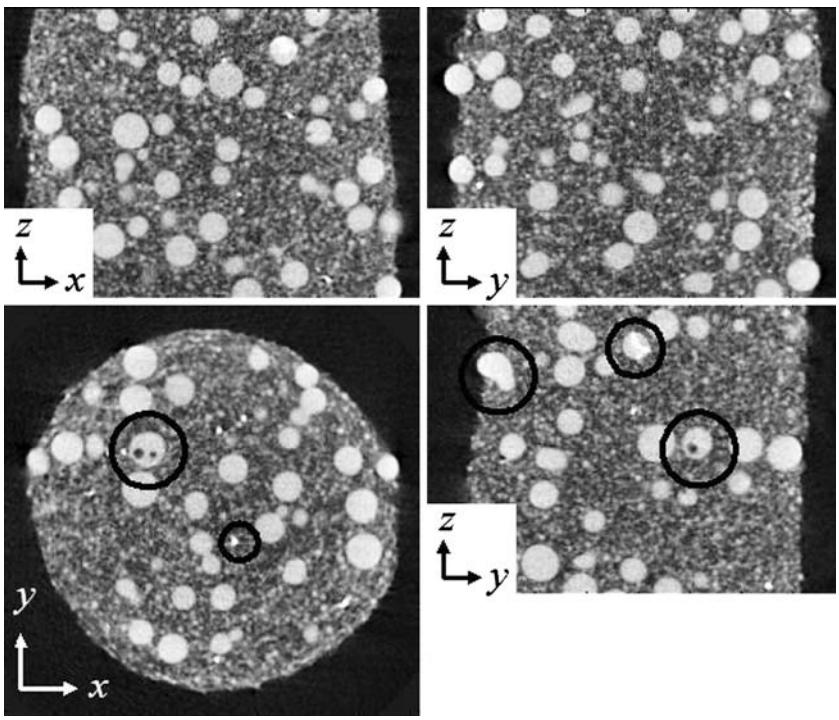

Fig. 3 Representative tomographic slices through the three orthogonal directions of the composite sample. The diameter of the sample is 5 mm

spheres and smaller ones embedded in the binder. A few brighter particles are observed, thought to be inclusions introduced into the material. The presence of voids within the glass spheres is also highlighted, although this was only in a few of the spheres. Also, a very small number of the particles were broken during processing of the material, prior to the shock tests. This would have an obvious effect on the shock wave as it travels through a broken particle, compared to that of an intact particle (as observed in the numerical simulation below). As so few particles were broken there would be negligible effect on the strength of the material under shock loading. Within the limits of the resolution of the XRT (ca. 5 μm), adhesion between the glass particles and the HTPB matrix was found to be better than that of the previous material that was studied [3], and for which tomography data of a shocked piece of the sample is shown in Fig. 5. There, shrinkage of the HTPB occurred as it hardened, thereby pulling away from the glass. The present overall microstructure can be considered to be three phase in nature, as shown by the histogram of the voxel grey level data in Fig. 4, comprising of glass particles, the HTPB matrix, and a small quantity of highly absorbing inclusions.

Final XRT

Greyscale tomography slices, extracted from the reconstructed 3D volume of a piece of glass composite material as scanned after the shock tests, are shown in Fig. 5. The top image shows a full vertical section through the dataset. It is noted that this shocked sample is from a batch where the 300 μm glass particles settled to the bottom of the container, as observed in the image, while the finer 30 μm particles remained dispersed throughout the sample. This is in contrast to the more recent batch, for which slices are shown in Fig. 3, where the larger particles are even dispersed throughout the sample. It is clear from Fig. 5 that large porous regions are also present in addition to the three phases observed previously, which is likely to have a modifying effect on the shock pulse as it moves through the material. In taking just the dense part, something representative of the bulk would be expected. Shown circled in the magnified images of Fig. 5 are broken glass particles. However, the number of broken particles was less than 5% within the larger impacted piece of material. Also, there is fine-grained debris inside the holes/cracks, which would suggest that some of the damage occurred prior to the shock tests.

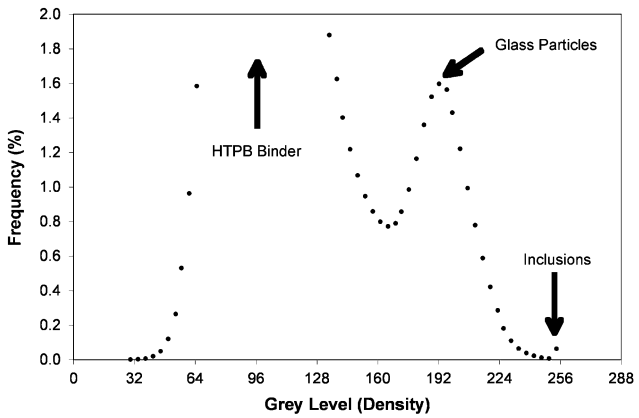

Fig. 4 Histogram showing the grey level distribution within the dataset and three phases—the binder, glass composite and inclusions

Shock data

Representative gauge traces from the plate impact experiments carried out on the composite material are presented in Fig. 6. The full matrix of other shots show similar behaviour and are analysed and plotted below. Table 2 shows the shot data for the full set of experiments carried out on the HTPB-Soda lime glass composite. The impact conditions for this shot are ca. 437 m s^{-1}, with a 10 mm Dural flyer plate.

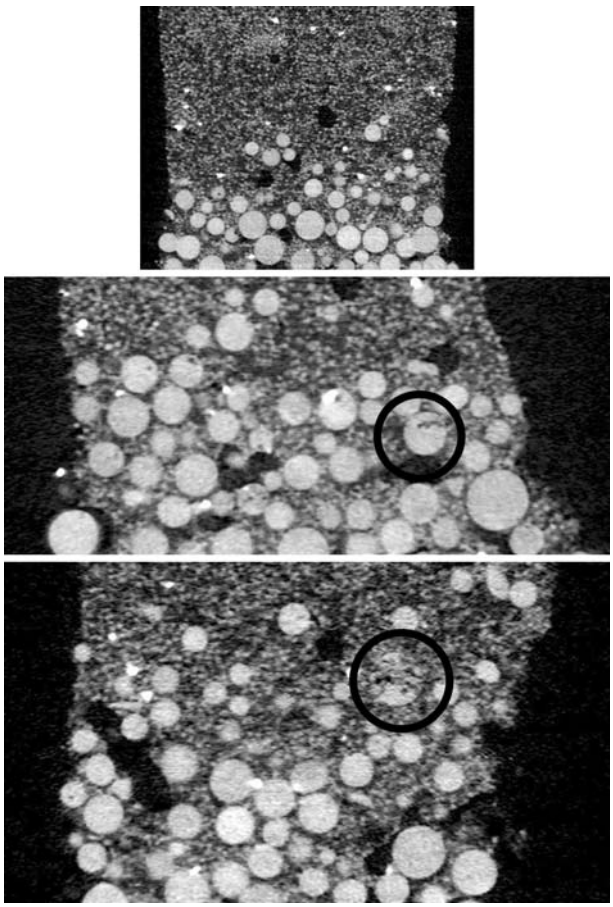

Fig. 5 Tomographic slices through an impacted piece of the composite material. The diameter of the sample is 5 mm

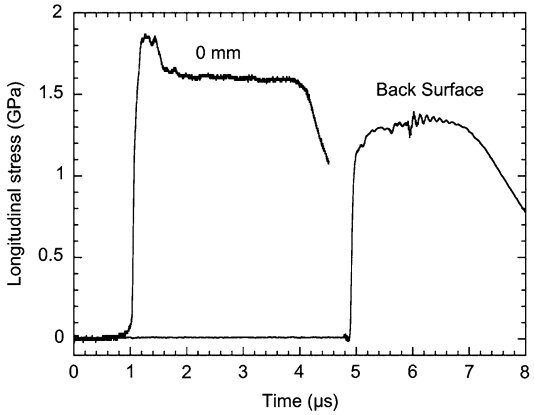

Fig. 6 Representative stress gauge traces from impact tests carried out on the composite. Tests were carried out using a 10 mm thick Dural flyer plate at 437 m s^{-1}

Table 2 Shot data for HTPB-Soda lime glass composite

v_{imp}(m/s)	u_p (mm/μs)	U_S (mm/μs)	Stress (GPa)
340	0.268	2.42	1.15
437	0.337	2.66	1.59
473	0.416	2.81	1.18
845	0.699	3.80	5.54

The initial overload pulse shown on the 0 mm trace (the trace measured by the embedded gauge), i.e., where the stress rises to 1.85 GPa and then drops, results from equilibration at the Dural coverplate. It can be seen that the stress measured at the 0 mm position is significantly higher than that measured by the back surface gauge, which was measuring the stress in the polymethylmethacrylate (PMMA) backing. This shows that there is a shock impedance mismatch with the PMMA in this shot—that of the composite is greater than that of PMMA, resulting in a higher stress amplitude. In other targets [3], where the density is the same for the same overall mixture, the magnitudes of both gauge traces are nearly identical, meaning that the Hugoniot of the composite and PMMA is similar. Apart from the magnitude, little can be determined from the embedded gauge since it is at the coverplate/composite interface. The back surface gauge, however, since it is monitoring the shock pulse after it has travelled through the composite, is more revealing. The temporal spacing between the gauge histories (Δt), in combination with the known gauge spacings (Δw) and target thickness, was used to determine the shock velocity ($U_s = \Delta w/\Delta t$). Using the later amplitude of the 0 mm trace (ca. 1.6 GPa), the shock velocity has been used in combination with the particle velocity (determined using impedance matching techniques) to produce the Hugoniot (equation of state) in stress-particle velocity space. These results are presented in Fig. 7. The composite appears to show a linear relation between U_s–u_p, conforming to the commonly accepted empirical relationship between shock velocity and particle velocity,

$$U_s = c_0 + Su_p \tag{1}$$

where c_0 and S are the shock parameters, the fitted values for which are shown in Fig. 7. This is in contrast to a previous study [3], which showed a nonlinear relationship, where a second-order polynomial in terms of particle velocity was fitted. The material manufactured for the points reproduced above was more uniform and better controlled than that used in [3]. This reduced porosity and better mixing resulted in a more uniform microstructure in the material from which these data were obtained. At low particle velocities this gave different results for the two materials but the two behaviours asymptote at higher particle velocities showing the hyrodynamics to be similar. It is likely that even the presence of a small amount of porosity has a modifying effect on the shock pulse as it moves through the material, causing a reduction in the shock velocity that is only overcome at higher shock stresses. Work must also be expended in closing this residual porosity as it collapses due to the shock.

It has been shown by Millett et al. for the soda-lime glass-HTPB system that the Hugoniot becomes steeper as the particle size increases [3]. Given the differences between impact stress and hydrodynamic pressure between the three different composite materials studied (coarse (300 μm glass beads), fine (30 μm beads) and mixed (consisting of equal proportions of 300 and 30 μm beads)), this suggests that the coarse composite has the highest shear strength, while the fine composite has the lowest. The reason for this is attributed to the coarse microstructure inhibiting flow, forcing it between the glass particles, or more likely is that it allows for sphere-to-sphere contact to occur much sooner under compression, thus increasing the

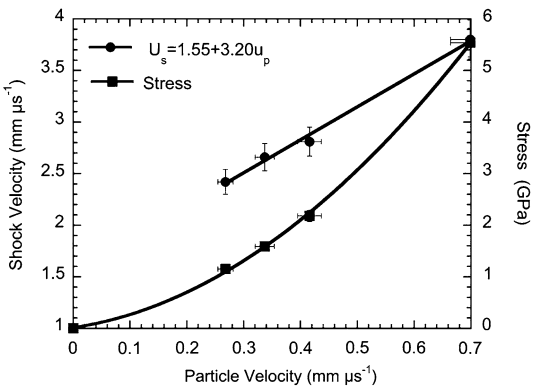

Fig. 7 Showing Hugoniots for the composite in σ_x–u_p and U_s–u_p space

shear strength. In the fine composite, the overall microstructure has greater ease in flowing as a whole. The hydrodynamic pressure (P_{HD}) is calculated according to,

$$P_{HD} = \rho_0 U_s u_p \tag{2}$$

where U_s is determined from Eq. (1), and is an average pressure as viewing the composite as a continuum. The stress measured by the gauges is expressed in terms of the hydrostatic pressure (P) and the materials shear strength (τ),

$$\sigma_x = P + \frac{4}{3}\tau \tag{3}$$

The differences between the measured stresses and the calculated hydrodynamic pressures can therefore give a useful indication of the variation of the shear strength of these composites. With all other factors being the same (ρ_0 and U_s–u_p), it appears that a composite with a large particle size is significantly stronger than one with a much finer distribution.

Numerical

Figure 8a shows a 3D representation of the reconstructed glass sphere interfaces, and Fig. 8b a square cross-sectioned portion of the full target that was used as the representative microstructure input to the hydrocode simulation. The spatial resolution of the reconstructed tomography dataset (ca. 5 μm) is sufficient to clearly identify the large spheres, while the smaller spheres are observed to form clusters.

Given this initial data as scanned prior to the impact tests, the hydrocode was used to carry out numerical impact experiments. In Fig. 9a a section of the sample at an early stage after it has been impacted into a rigid wall at the base of the calculation is shown. In this figure a square cross section sample of the data has been extracted and rigid boundary conditions have been applied at the edges and inflow boundary conditions at the top. The whole sample was subjected to an initial applied velocity of 1,000 m s^{-1} into the rigid wall. The reconstruction of the glass spheres in the binder in the unshocked region as well as the early stages of the shock wave moving back from the impact face is illustrated. Figure 9b shows the density contours at a later stage. The shock has progressed through the composite and significant structure is apparent. From Fig. 9a and b it is observed that the shock front is not planar. The elastic fronts travel fastest through the soda-lime glass particles owing to a higher longitudinal sound speed, c_L (see Table 1). The lower wave speed through the HTPB makes this phase slower to equilibrate pressure. The non-planarity is of the order of 100 μm, indicating a sweep

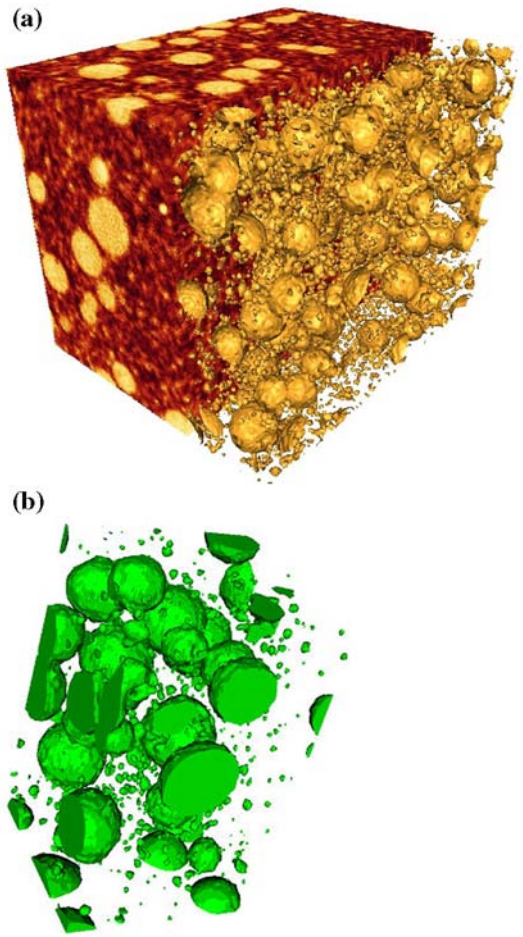

Fig. 8 (**a**) 3 D reconstruction from the X-ray images of the glass particles (gold) within the polymer binder (red). (**b**) Showing the glass particles in the sample of the target, as the input to the hydrocode simulation. The larger glass spheres are 300 μm in diameter

time of the gauge package of the order of its response time. This emphasises the inhomogeneity of the flow at this length scale. The flow is fully three-dimensional at the mesoscale. Shock diffraction around the particles is also observed.

A real 1D file has been used as input for the hydrocode. Non-equilibrium pressure and particle velocity is observed from the model, which provides a continuum measurement of stress/shock velocity. This analysis complements alternative means of diagnosing the shock properties in a composite [19]. Details of the shock interaction on the mesoscale are important in understanding ignition processes.

Conclusions

X-ray microtomography has been used in a first step to investigate the microstructure of a plastic bonded explosive analogue and to link this microstructure to simulation of

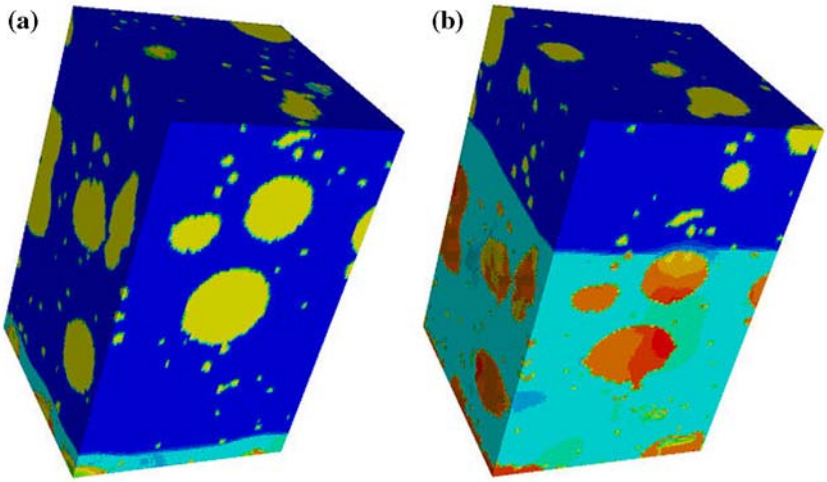

Fig. 9 Density plots of the same section of the sample as in Fig. 8b showing an a. early and b. later stage of a 1,000 m s^{-1} impact. The larger glass spheres are 300 μm in diameter

mechanical response. The technique has been developed and is shown to be suited to such a study of the phases present within and how they respond to mechanical deformation. The sample used in the present study for the shock tests had been prepared for that shot and so is not representative of actual target conditions. This is something to be improved in further work. A valid 1D particle velocity (strain) continuum model has been constructed, which captures details of the microstructural response, but at the mesoscale and fully 3D. The work has provided a direct link between microstructural analysis, experimental investigation and numerical simulation. Effort was put into both resolving features at appropriate length scales, and into reading these across onto the numerical platform. Shock data has been gathered for the composite and differs from that collected for a similar material previously [3]. The local shock response of this class of materials is sensitive to the distribution of phases within the microstructure. Our aim is to complete studies on this inert stimulant and then move towards applying the same techniques to real explosive samples.

In terms of furthering this work, finer resolution XRT will allow us to detect the presence of very small fines within such materials. The processing of the targets will be improved, as will the recovery of the material. The aim would also be to fully quantitatively analyse the processes occurring in the model of the data.

Acknowledgements We gratefully acknowledge the support of Dr. Peter Barnes of the UK Defence Ordnance Safety Group (DOSG) who funded part of this work.

References

1. Bourne NK, Milne AM (2003) Proc R Soc Lond A 459:1851
2. Millett JCF, Bourne NK (2004) J Phys D: Appl Phys 37:2613
3. Millett JCF, Bourne NK, Akhavan J, Milne AM (2005) J Appl Phys 97:043524
4. Copley DC, Eberhard JW, Mohr GA (1994) J Mat 46(1):14
5. Peix G, Duvauchelle P, Freud N (2000) In: Baruchel J, Buffière J-Y, Maire E, Merle P, Peix G (eds) X-ray tomography in materials science. HERMES Science Publications, Paris, p 15
6. Stock SR (1999) Int Mat Rev 44:141
7. Baer MR, Trott WM (2002) In: Furnish MD, Thadhani NN, Horie Y (eds) Shock compression of condensed matter (2001). American Institute of Physics, Melville, NY, p 713
8. Trott WM, Casteñada JN, O'Hare JJ, Knudson MD, Chhabildas LC, Baer MR, Asay JR (2001) In: Staudhammer KP, Murr LE, Meyers MA (eds) Fundamental issues and applications of shock-wave and high-strain-rate phenomena. Elsevier, New York, p 647
9. Mas EM, Clements BE (2001) J Appl Phys 90:5535
10. Millett JCF, Bourne NK, Akhavan J (2004) J Appl Phys 95:4722
11. Bourne NK, Millett JCF, Rosenberg Z, Murray N (1998) J Mech Phys Solids 46:1887
12. Feldkamp LA, Davis LC, Kress JW (1984) J Opt Sci 1:612
13. Bourne NK (2003) Meas Sci Technol 14:273
14. Bourne NK, Stevens GS (2001) Rev Sci Instrum 72:2214
15. Millett JCF, Bourne NK (2001) J Appl Phys 89:2576
16. Rosenberg Z, Yaziv D, Partom Y (1980) J Appl Phys 51:3702
17. Marsh SP (1980) LASL shock Hugoniot data. University of California Press, Los Angeles
18. Milne AM (2004) EDEN user manual. Fluid Gravity Engineering Ltd., St. Andrews, UK
19. Milne AM, Bourne NK, Millett JCF (2005) In: Furnish MD, Elert M, Russell TP, White CT (eds) Shock compression of condensed matter. American Institute of Physics, Melville, NY, p 175